

AN *HST* STUDY OF THE SUPERNOVAE ACCOMPANYING GRB 040924 AND GRB 041006

A. M. SODERBERG,¹ S. R. KULKARNI,¹ P. A. PRICE,² D. B. FOX,¹ E. BERGER,^{3,4,5} D.-S. MOON,^{6,7} S. B. CENKO,⁶
 A. GAL-YAM,^{1,5} D. A. FRAIL,⁸ R. A. CHEVALIER,⁹ L. COWIE,² G. S. DA COSTA,¹⁰ A. MACFADYEN,¹
 P. J. MCCARTHY,³ N. NOEL,¹¹ H. S. PARK,¹² B. A. PETERSON,¹⁰ M. M. PHILLIPS,³
 M. RAUCH,³ A. REST,¹³ J. RICH,¹⁰ K. ROTH,¹⁴ M. ROTH,³ B. P. SCHMIDT,¹⁰
 R. C. SMITH,¹³ AND P. R. WOOD¹⁰

Received 2005 April 18; accepted 2005 September 12

ABSTRACT

We present the results from a *Hubble Space Telescope* ACS study of the supernovae (SNe) associated with gamma-ray bursts (GRBs) 040924 ($z = 0.86$) and 041006 ($z = 0.71$). We find evidence that both GRBs were associated with an SN 1998bw-like supernova dimmed by ~ 1.5 and ~ 0.3 mag, respectively, making GRB 040924 the faintest GRB-associated SN ever detected. We study the luminosity dispersion in GRB/XRF-associated SNe and compare to local Type Ibc SNe from the literature. We find significant overlap between the two samples, suggesting that GRB/XRF-associated SNe are not necessarily more luminous and do not necessarily produce more ^{56}Ni than local SNe. Based on the current (limited) data sets, we find that the two samples may share a similar ^{56}Ni production mechanism.

Subject headings: gamma rays: bursts — radiation mechanisms: nonthermal — supernovae: general

1. INTRODUCTION

Gamma-ray burst (GRB) explosions harbor both spherical supernova (SN) ejecta and highly collimated engine-driven jets (Galama et al. 1998; Matheson et al. 2003; Hjorth et al. 2003). This “spherical+jet” paradigm for the geometry of GRBs implies that both explosion components must be studied independently. Early ($t \lesssim$ few days) optical observations trace the synchrotron radiation produced from the engine-driven relativistic jets, while late-time ($t \gtrsim 20$ days) observations probe the optical emission from the nonrelativistic spherical SN ejecta, powered by the decay of ^{56}Ni . Such observations allow us to address the following fundamental questions regarding the GRB/SN connection: what is the diversity among GRB-associated SNe, and how does the sample compare to local Type Ibc supernovae (SNe Ibc)?

Three of the best-studied events, SNe 1998bw, 2003dh, and 2003lw (associated with GRBs 980425, 030329, and 031203, respectively) were strikingly similar, with brighter optical luminos-

ities and faster photospheric velocities than local SNe Ibc (Galama et al. 1998; Patat et al. 2001; Matheson et al. 2003; Hjorth et al. 2003; Malesani et al. 2004). These events suggested that the SNe associated with GRBs belong to a distinct subclass of “hyper-energetic” SNe. However, there are also several counterexamples: underluminous SNe associated with GRBs and X-ray flashes (XRFs; events very similar to GRBs but differentiated by a soft prompt energy release peaking in the X-ray band; Heise et al. 2001) with optical luminosities significantly fainter than SN 1998bw. The most extreme examples are GRB 010921 (Price et al. 2003; but see Zeh et al. 2004) and XRF 040701 (Soderberg et al. 2005b), for which the associated SNe are at least 1.3 and 3.2 mag fainter than SN 1998bw, respectively.

Motivated by our fundamental questions, we began a *Hubble Space Telescope* (*HST*) program to study the diversity in SNe associated with GRBs and XRFs (GO-10135; PI: Kulkarni). In Soderberg et al. (2005b), we presented the results of our *HST* SN search in XRFs 020903, 040701, 040812, and 040916. We showed that at least some XRFs are associated with SNe, but that there may be a significant dispersion in their optical peak magnitudes.

Here we present the results from our *HST* study of the SNe associated with GRBs 040924 ($z = 0.86$) and 041006 ($z = 0.71$). In § 3 we show that each is associated with an SN 1998bw-like SN dimmed by ~ 1.5 and ~ 0.3 mag, respectively, making GRB 040924 the faintest GRB-associated SN detected to date. These two events suggest a notable dispersion of peak optical magnitudes for GRB-associated SNe.

Finally, we compile optical peak magnitudes and ^{56}Ni mass estimates for all GRB/XRF-associated SNe and local SNe Ibc to study the diversity among these two samples. In § 4 we address the question of whether both samples are drawn from the same parent population of core-collapse SNe.

2. SN LIGHT-CURVE SYNTHESIS

In modeling the GRB-associated SNe, we adopted optical data for the local SNe 1994I (Richmond et al. 1996), 1998bw (Galama et al. 1998; McKenzie & Schaefer 1999), and 2002ap (Foley et al.

¹ Division of Physics, Mathematics, and Astronomy, 105-24, California Institute of Technology, Pasadena, CA 91125.

² University of Hawaii, Institute of Astronomy, 2680 Woodlawn Drive, Honolulu, HI 96822-1897.

³ Observatories of the Carnegie Institution of Washington, 813 Santa Barbara Street, Pasadena, CA 91101.

⁴ Department of Astrophysical Sciences, Princeton University, Princeton, NJ 08544.

⁵ Hubble Fellow.

⁶ Space Radiation Laboratory 220-47, California Institute of Technology, Pasadena, CA 91125.

⁷ Robert A. Millikan Fellow.

⁸ National Radio Astronomy Observatory, Socorro, NM 87801.

⁹ Department of Astronomy, University of Virginia, P.O. Box 3818, Charlottesville, VA 22903-0818.

¹⁰ Research School of Astronomy and Astrophysics, The Australian National University, Weston Creek, ACT 2611, Australia.

¹¹ Instituto de Astrofísica de Canarias, C/Vía Lactea s/n, E-38200, La Laguna, Tenerife, Spain.

¹² Lawrence Livermore National Laboratory, 7000 East Avenue, Livermore, CA 94550.

¹³ Cerro Tololo Inter-American Observatory, Casilla 603, La Serena, Chile.

¹⁴ Gemini Observatory, 670 North A’ohoku Place, Hilo, HI 96720.

TABLE 1
HST OBSERVATION LOG

Target	Observation Date (UT)	Δt (day)	Exposure Time (s)	Filter	HST Magnitude (AB) ^a	Extinction (A_i) ^b	Johnson Magnitude (Vega) ^c
GRB 040924.....	2004 Nov 2.4	38.9	3064	F775W	26.44 ± 0.23	$A_I = 0.113$	$I = 25.75 \pm 0.23$
	2004 Nov 2.5	39.0	3211	F850LP	25.60 ± 0.11	$A_z = 0.106$	$z = 24.96 \pm 0.11$
	2004 Nov 26.5	63.0	3932	F775W	>27.59	$A_I = 0.113$	$I > 26.90$
	2005 Feb 18.5	147.0	3932	F775W
	2005 Feb 19.5	148.0	3932	F850LP
GRB 041006.....	2004 Nov 2.3	26.7	3832	F775W	24.01 ± 0.05	$A_I = 0.044$	$I = 23.47 \pm 0.05$
	2004 Nov 2.3	26.7	3430	F850LP	23.58 ± 0.04	$A_z = 0.041$	$z = 23.01 \pm 0.04$
	2004 Nov 27.4	51.9	4224	F775W	25.11 ± 0.10	$A_I = 0.044$	$I = 24.57 \pm 0.10$
	2004 Dec 23.4	77.8	4224	F775W	25.83 ± 0.19	$A_I = 0.044$	$I = 25.29 \pm 0.19$
	2005 Feb 10.3	126.8	4224	F775W	26.26 ± 0.25	$A_I = 0.044$	$I = 25.73 \pm 0.25$
	2005 Feb 11.2	127.7	4224	F850LP	25.90 ± 0.21	$A_z = 0.041$	$z = 25.32 \pm 0.21$

^a AB system magnitudes in the *HST* filters given in the fifth column. Photometry was done on residual images (see § 3). We have assumed the source flux to be negligible in the final (template) epoch for GRB 040924. For GRB 041006, we estimated the source flux in the template epoch using PSF photometry and corrected the residual photometry accordingly. All represent observed magnitudes, not corrected for foreground extinction.

^b Galactic extinction from Schlegel et al. (1998).

^c Magnitudes from the sixth column, converted to the Vega system and corrected for foreground extinction using A_z given in the seventh column.

2003) as templates. These three SNe were selected on the basis of their well-sampled optical light curves, which represent an overall spread in the observed properties of Type Ibc SNe. To produce synthesized light curves for each of these template SNe, we compiled optical *UBVR* observations from the literature and smoothed the extinction-corrected (foreground plus host galaxy) light curves. We then redshifted the light curves by interpolating over the photometric spectrum and stretching the arrival time of the photons by a factor of $(1+z)$. The details of each template data set are described in Soderberg et al. (2005b).

3. HST GRB-SN SEARCH

Using the Wide-Field Camera (WFC) of the Advanced Camera for Surveys (ACS) on board *HST*, we imaged the fields of GRBs 040924 and 041006. For each target we undertook observations at several epochs, spanning $t \sim 30$ and ~ 150 days, in order to search for optical emission associated with an underlying SN. Each epoch consisted of 2–4 orbits, during which we imaged the field in filters, F775W and/or F850LP, corresponding to SDSS i' and z' bands, respectively.

The *HST* data were processed using the *multidriz* routine (Fruchter & Hook 2002) within the *stdas* package of IRAF. Images were drizzled using *pixfrac* = 0.8 and *pixscale* = 1.0, resulting in a final pixel scale of $0''.05 \text{ pixel}^{-1}$. Drizzled images were then registered to the first epoch using the *xregister* package in IRAF.

To search for source variability and remove host galaxy contamination, we used the ISIS subtraction routine by Alard (2000), which accounts for temporal variations in the stellar point-spread function (PSF). Adopting the final epoch observations as template images, we produced residual images. These residual images were examined for positive sources positionally coincident with the afterglow error circle. To test our efficiency at recovering faint transient sources, false stars with a range of magnitudes were inserted into the first-epoch images using IRAF task *mkobject*. The false stars were overlayed on top of the diffuse host galaxy emission at radial distances similar to that measured for the afterglow. An examination of the false stellar residuals provided an estimate of the magnitude limit (3σ) to which we could reliably recover faint transients.

Photometry was performed on the residual sources within a $0''.5$ aperture. We converted the photometric measurements to in-

finite aperture and calculated the corresponding AB magnitudes within the native *HST* filters using the aperture corrections and zero points provided by Sirianni et al. (2005). For comparison with ground-based data, we also converted the photometric measurements to Johnson I - and z -band (Vega) magnitudes using the transformation coefficients derived by Sirianni et al. (2005) and adopting the source color given by the first-epoch F775W and F850LP observations.

In the following sections we summarize the afterglow properties for both targets and the photometry derived from our *HST* SN study. A log of the *HST* observations for the GRBs follows in Table 1.

3.1. GRB 040924

3.1.1. Prompt Emission and Afterglow Properties

GRB 040924 was detected by the Wide-Field X-Ray Monitor (WXM) on-board the *High Energy Transient Explorer 2* (HETE-2) satellite on 2004 September 24.4951 UT. Preliminary analysis showed the peak of the spectral energy distribution was soft, $E_{\text{peak}} \approx 42 \pm 6 \text{ keV}$, and the ratio of X-ray (7–30 keV) to gamma-ray (30–400 keV) fluence, $S_X/S_\gamma \approx 0.6$, classifying this event as an X-ray-rich burst (Fenimore et al. 2004). Using the Robotized Palomar 60 inch (1.52 m) telescope (P60; S. B. Cenko et al. 2006, in preparation), we discovered the optical afterglow at position $\alpha = 02^{\text{h}}06^{\text{m}}22^{\text{s}}.55$, $\delta = +16^\circ 06' 48''.8$ (J2000.0) with an uncertainty of $0''.2$ in each coordinate (Fox 2004), well within the $6''.4$ (radius) localization region. As shown by our extensive P60 monitoring, the afterglow was $R \approx 18.0 \text{ mag}$ at $t \approx 16$ minutes and subsequently decayed.

We continued to monitor the afterglow emission from $t \approx 0.01$ to $t \approx 1$ day after the burst (Table 2), producing a well-sampled R -band light curve. As shown in Figure 2, these data show a shallow initial decay, followed by a steepening at $t \sim 0.02$ days. In an effort to characterize the light-curve behavior, we fit a smoothed, broken power-law model (e.g., Beuermann et al. 1999) of the form

$$F_\nu(t) = 2F_{\nu,0} \left[\left(\frac{t}{t_b} \right)^{\alpha_1 s} + \left(\frac{t}{t_b} \right)^{\alpha_2 s} \right]^{-1/s}, \quad (1)$$

where t_b is the break time in days, $F_{\nu,0}$ is the normalized flux density at $t = t_b$, and α_1 and α_2 are the asymptotic indices at $t \ll t_b$ and

TABLE 2
PALOMAR 60 INCH *R*-BAND OBSERVATIONS OF GRB 040924

Observation Date (UT)	Δt (day)	Magnitude ^a
2004 Sep 24.506.....	0.011	17.8 ± 0.1
2004 Sep 24.509.....	0.014	17.9 ± 0.1
2004 Sep 24.512.....	0.017	18.0 ± 0.1
2004 Sep 24.513.....	0.018	18.1 ± 0.1
2004 Sep 24.514.....	0.019	18.0 ± 0.1
2004 Sep 24.517.....	0.022	18.1 ± 0.1
2004 Sep 24.519.....	0.024	18.2 ± 0.1
2004 Sep 24.526.....	0.030	18.5 ± 0.1
2004 Sep 24.527.....	0.032	18.5 ± 0.1
2004 Sep 24.530.....	0.035	18.6 ± 0.1
2004 Sep 24.539.....	0.044	19.0 ± 0.1
2004 Sep 24.875.....	0.380	21.9 ± 0.1
2004 Sep 24.894.....	0.399	22.1 ± 0.1
2004 Sep 24.909.....	0.414	22.2 ± 0.1
2004 Sep 24.926.....	0.430	22.1 ± 0.1
2004 Sep 24.942.....	0.447	22.2 ± 0.1
2004 Sep 24.957.....	0.462	22.3 ± 0.1
2004 Sep 24.972.....	0.477	22.3 ± 0.1
2004 Sep 24.988.....	0.493	22.2 ± 0.1
2004 Sep 25.003.....	0.508	22.4 ± 0.1
2004 Sep 25.018.....	0.523	22.5 ± 0.1
2004 Sep 25.036.....	0.540	22.5 ± 0.1
2004 Sep 25.050.....	0.555	22.7 ± 0.1
2004 Sep 25.066.....	0.571	22.6 ± 0.1
2004 Sep 25.081.....	0.586	22.4 ± 0.1
2004 Sep 25.097.....	0.602	22.4 ± 0.1
2004 Sep 25.224.....	0.729	22.6 ± 0.1

^a Corrected for Galactic extinction according to Schlegel et al. (1998).

$t \gg t_b$, respectively. Here s is used to parameterize the sharpness of the break. A best fit ($\chi_r^2 = 3.3$) is found for the following parameters: $F_{\nu,0} \approx 90.4 \mu\text{Jy}$, $\alpha_1 \approx 0.39$, $\alpha_2 \approx 1.22$, $t_b \approx 0.021$ days, and $s \approx 10$. To interpret this steepening as a jet break (Rhoads 1999; Sari et al. 1999) would imply a electron spectral index, $N \propto \gamma^{-p}$ with $p \approx 1.2$. This value is significantly lower than those typically observed ($p \approx 2.2$; Yost et al. 2003) and far below the range predicted by the standard blast wave model, $p = [2-3]$ (Sari et al. 1998). We therefore ascribe this early afterglow phase (and steepening) to another process, perhaps similar to that observed for the initial slow decay of GRB 021004 (Fox et al. 2003), interpreted as interaction with a stellar wind medium (Li & Chevalier 2003).

Terada & Akiyama (2004) report that the afterglow was $K \approx 17.5 \pm 0.1$ mag at $t \approx 0.1$ days. Comparison with the *R*-band afterglow model at the same epoch provides a spectral index, $F_\nu \propto \nu^\beta$ with $\beta \approx -0.7$, between the *R* and *K* bands. Adopting this spectral index, we interpolate our *R*-band afterglow model to the *I* and *z* bands for comparison with our late-time *HST* observations (§ 3.1.2).

Optical spectroscopy later revealed that the burst was located at a redshift of $z = 0.859$, based on identification of several host galaxy emission lines (Wiersema et al. 2004).

3.1.2. *HST* Observations

HST ACS imaging was carried out on 2004 November 2.4 and 26.5 and 2005 February 19.0 UT ($t \approx 39, 63$, and 147 days after the burst). For the first and third epochs, we observed with both the F775W and F850LP filters, while the second epoch consisted of just F775W observations. We astrometrically tied

the *HST* and P60 images using four sources in common, which results in a final systematic uncertainty of $0''.22$ (2σ).

Our *HST* observations reveal that the optical afterglow error circle coincides with a strongly variable source at $\alpha = 02^h06^m22^s552$, $\delta = +16^\circ06'49''.11$ (J2000.0), lying $\sim 0''.3$ north-west of the host galaxy nucleus. We interpret this source as a combination of afterglow plus SN emission. Figure 1 shows the first epoch, template image and first-epoch residual for both the F775W and F850LP filter observations. There is no evidence for a point source in our third-epoch (template) images. We therefore make the reasonable assumption that the transient source flux is negligible at that time. The resulting *HST* photometry is listed in Table 1.

Figure 2 shows the *HST* photometry along with our *I*- and *z*-band afterglow models (see § 3.1.1) and some early-time data compiled from GRB Coordinates Network circulars (GCNs; Silvey et al. 2004), all corrected for Galactic extinction. By comparing the afterglow models with the *HST* photometry, we find evidence for a ~ 1.9 mag rebrightening at $t \sim 39$ days. We note that the timescale of this rebrightening is roughly consistent with the peak time of SN 1998bw at $z = 0.86$.

3.1.3. Associated SN

We interpret the observed late-time rebrightening as an associated SN component. Comparison with our synthesized (redshifted) SN light curves reveals that an associated SN 1998bw–like SN would be ~ 1.5 mag brighter than the *HST* observation at $t \sim 39$ days, while SN 1994I and SN 2002ap–like light curves are fainter by ~ 0.8 and ~ 1.5 mag, respectively. To fit the *HST* observations, we add the contribution from a template SN light curve (see § 2) to the afterglow model. We allow the brightness of the synthesized template to be scaled but do not allow for the light curve to be stretched. Moreover, we assume that the GRB and SN exploded at the same time. By fitting the *HST* *I*- and *z*-band data simultaneously, we find a best-fit solution ($\chi_r^2 \approx 0.8$) for an SN 1998bw–like SN dimmed by ~ 1.5 mag (Fig. 2). We note that on this timescale, the SN emission clearly dominates that of the afterglow model. Therefore, even if the afterglow underwent a late-time ($t > 2$ days) jet break, our SN fits would not be significantly affected.

Host galaxy extinction could affect our SN light-curve fits since it implies that the associated SN was more luminous than the observations suggest. Fortunately, we can constrain the host galaxy extinction using optical/IR afterglow observations, since extinction will produce an artificial steepening of the synchrotron spectrum. Making the reasonable assumption that the synchrotron cooling frequency was above the optical/IR bands at early time, we have $\beta_{\text{opt/IR}} \approx -0.7 = -(p-1)/2$ and thus $p \approx 2.4$. For $p < 2$ the standard blast wave model is violated, therefore implying that the spectral index must be steeper than $\beta_{\text{opt/IR}} = -0.5$. Adopting this limit for the intrinsic spectral index of the afterglow implies a constraint on the host galaxy extinction of $A_{V,\text{host}} \lesssim 0.16$ mag. This corresponds to limits on the observed extinction of $A_I \approx A_z \lesssim 0.20$ mag, implying that the associated SN was at least 1.3 mag fainter than SN 1998bw. We therefore conclude that the SN associated with GRB 040924 was between 1.3 and 1.5 mag fainter than SN 1998bw at maximum light, making this event the faintest GRB-associated SN ever detected.

3.2. GRB 041006

3.2.1. Prompt Emission and Afterglow Properties

GRB 041006 was discovered by the *HETE-2* WXM on 2004 October 6.513 UT. The ratio of 2–30 and 30–400 keV channel

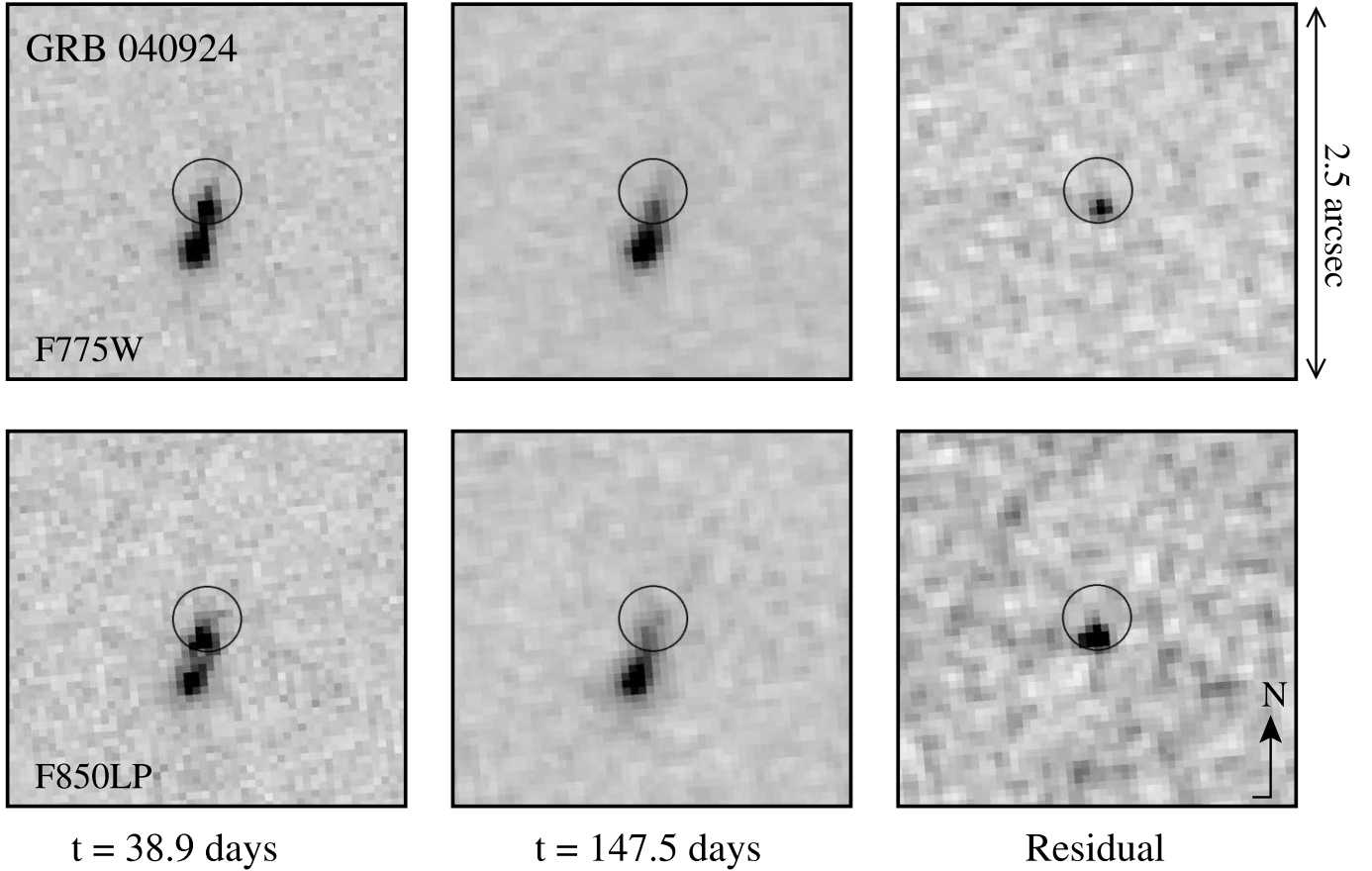


FIG. 1.—Six-panel frame showing *HST* ACS imaging for GRB 040924 at $t \sim 38.9$ days (epoch 1) and $t \sim 147.5$ days (epoch 3) in the F775W and F850LP filters. By subtracting epoch 3 images from those of epoch 1, we produced the residual images shown above. We have applied the same stretch to all frames. As clearly shown in the residual images, a transient source is detected coincident with the $0''.22$ (2σ) optical afterglow position (circle).

fluences showed the event was an X-ray–rich burst. The event was localized to a $5''.0$ (radius) localization region centered at $\alpha = 00^{\text{h}}54^{\text{m}}53^{\text{s}}$, $\delta = +01^{\circ}12'04''$ (J2000.0; Galassi et al. 2004).

Using the Siding Springs Observatory (SSO) 40 inch (1.02 m) telescope, we discovered the optical afterglow at $\alpha = 00^{\text{h}}54^{\text{m}}50^{\text{s}}.17$, $\delta = +01^{\circ}14'07''.0$ (J2000.0; Da Costa et al. 2004), consistent with the *HETE-2* error circle. As our early-time ($t \approx 0.024$ – 0.122 days; Table 3) SSO 40 inch and 2.3 m observations show, the afterglow was $V \approx 18.1$ mag at $t \approx 35$ minutes and subsequently faded in the B , V , and H bands.

Stanek et al. (2005) have presented an extensive compilation of (extinction-corrected) R -band afterglow data from $t \approx 0.03$ to $t \approx 64$ days, primarily from the MMT and from the GCNs (see references therein). They fit the evolution of the early light curve (up to $t \sim 4$ days) with the broken power-law model given in equation (1), finding best-fit parameters of $F_{\nu,0} \approx 50.0 \mu\text{Jy}$, $\alpha_1 \approx 0.57$, $\alpha_2 \approx 1.29$, $t_b \approx 0.14$ days, and $s \approx 2.59$. As in the case of GRB 040924 (§ 3.1.1), this observed steepening is too shallow to be interpreted as a jet break under the standard blast wave model. We instead interpret this early afterglow phase as due to another process, possibly the result of an off-axis viewing angle as proposed by Granot et al. (2005).

Combining our early-time SSO data with those compiled by Stanek et al. (2005), we estimate the spectral index of the optical/IR afterglow to be $\beta_{\text{opt/IR}} \approx -0.5$ by fitting a power law to the B -, V -, R -, and H -band data. Adopting this spectral index, we interpolate the R -band model to the I and z bands for comparison with our late-time *HST* observations (§ 3.2.2).

Optical spectroscopy at $t \approx 0.6$ days revealed that the burst was located at $z \geq 0.712$, based on tentative identification of several absorption lines in the low signal-to-noise spectrum (Fugazza et al. 2004). To confirm this redshift measurement, we acquired a spectrum of the optical afterglow with the Gemini Multi-Object Spectrograph (GMOS) on Gemini North (GN-2004B-Q-5; PI: Price) commencing at 2004 October 7.36 UT ($t \approx 0.85$ days). Using the R400 grating and a $1''$ slit, we obtained four individual 1800 s exposures. Data were reduced and extracted using the `gemini.gmos` package in IRAF. We identify four absorption lines and one emission line (Table 4 and Fig. 3), which we interpret as arising from Mg II, Ca II, and [O II] at a redshift of $z = 0.716$, in broad agreement with the earlier measurement by Fugazza et al. (2004). Based on the high equivalent widths and the presence of [O II], this is likely the redshift of the host galaxy, and not due to an intervening system along the line of sight. Using the R -band afterglow model and the photometrically derived spectral index, we flux calibrate the spectrum and obtain an approximate [O II] emission line flux of $1.3 \times 10^{-17} \text{ ergs cm}^{-2} \text{ s}^{-1}$. Adopting the conversion factor of Kennicutt (1998), this line flux corresponds to a star formation rate of $0.5 M_{\odot} \text{ yr}^{-1}$ at the redshift of the host galaxy.¹⁵

3.2.2. *HST* Observations

HST ACS imaging was carried out on 2004 November 2.3 and 27.4, 2004 December 23.4, and 2005 February 10.5 UT

¹⁵ We have adopted a cosmology with $H_0 = 65 \text{ km s}^{-1} \text{ Mpc}^{-1}$ and $(\Omega_M, \Omega_{\Lambda}) = (0.3, 0.7)$.

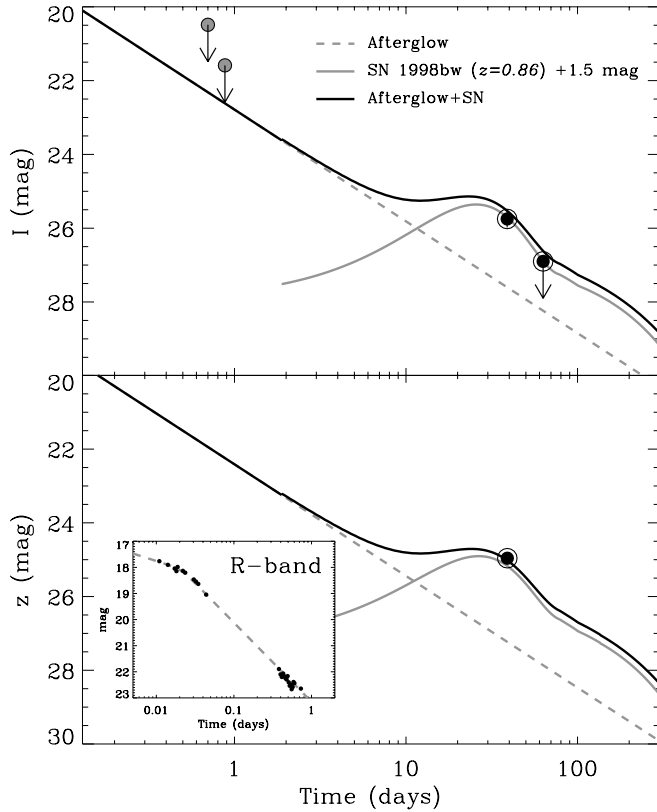


FIG. 2.—Constraints on a SN associated with GRB 040924. As discussed in § 3.1.1, we fit a broken power-law model to our P60 *R*-band afterglow data reported in Table 2 (inset). Adopting a spectral index of $\beta \approx -0.7$, we then extrapolate the *R*-band afterglow fit to the *I* and *z* bands (gray dashed lines). Extinction-corrected data have been compiled from the GCNs and are overplotted (gray arrows; Silvey et al. 2004). We fit the late-time *HST* data (circled dots) by summing the contribution from the afterglow model plus that from a SN. We find a best-fit (solid black lines) by including an SN 1998bw-like SN (gray solid lines) redshifted to $z = 0.86$ and dimmed by ~ 1.5 mag.

TABLE 3
SSO 40 INCH AND 2.3 m OBSERVATIONS OF GRB 041006

Observation Date (UT)	Δt (days)	Filter	Telescope	Magnitude ^a
2004 Oct 6.537	0.024	<i>V</i>	40 inch	18.11 ± 0.02
2004 Oct 6.541	0.028	<i>V</i>	40 inch	18.20 ± 0.04
2004 Oct 6.546	0.033	<i>V</i>	40 inch	18.29 ± 0.02
2004 Oct 6.550	0.037	<i>V</i>	40 inch	18.38 ± 0.03
2004 Oct 6.555	0.042	<i>V</i>	40 inch	18.48 ± 0.03
2004 Oct 6.582	0.069	<i>B</i>	40 inch	19.18 ± 0.07
2004 Oct 6.586	0.073	<i>B</i>	40 inch	19.24 ± 0.06
2004 Oct 6.590	0.077	<i>B</i>	40 inch	19.29 ± 0.07
2004 Oct 6.595	0.082	<i>V</i>	40 inch	18.99 ± 0.03
2004 Oct 6.605	0.092	<i>H</i>	2.3 m	17.16 ± 0.07
2004 Oct 6.612	0.099	<i>H</i>	2.3 m	17.12 ± 0.06
2004 Oct 6.620	0.107	<i>H</i>	2.3 m	17.19 ± 0.06
2004 Oct 6.627	0.114	<i>H</i>	2.3 m	17.47 ± 0.06
2004 Oct 6.635	0.122	<i>H</i>	2.3 m	17.43 ± 0.07

^a Corrected for Galactic extinction according to Schlegel et al. (1998). *B*- and *V*-band photometry is relative to the field calibration by Henden (2004) while the *H*-band photometry is relative to 2MASS.

TABLE 4
GRB 041006 SPECTROSCOPIC LINES

Observed Wavelength (Å)	Equivalent Width (Å)	Line Identification	Rest Wavelength (Å)
4798.16.....	4.4	Mg II	2796
4810.35.....	3.9	Mg II	2803
6396.31.....	1.7	O II	3727
6750.32.....	1.4	Ca II	3935
6810.06.....	1.1	Ca II	3970

($t \approx 27, 52, 78$, and 127 days after the burst). For the first and fourth epochs, we observed with both the F775W and F850LP filters, while the second and third epochs consisted of just F775W observations. We astrometrically tied the *HST* and SSO images using five sources in common, resulting in a final systematic uncertainty of $0''.53$ (2σ).

Our *HST* observations reveal that the optical afterglow error circle coincides with a strongly variable source at $\alpha = 00^h54^m50^s229$, $\delta = +01^\circ14'05''.82$ (J2000.0). The source is situated directly on top of a faint host galaxy, which is at the detection limit of our *HST* images. We note the presence of a brighter galaxy $\sim 1''$ from the afterglow position, which was misidentified as the host galaxy by Covino et al. (2004) on the basis of ground-based images.

Figure 4 shows the first epoch, template image, and first-epoch residual for both the F775W and F850LP filter observations. From the figure, it is clear that the source is still faintly detected in our final epoch (template) observations. To assume negligible source flux in the template images is therefore not valid. We estimate the flux of the source in our template images by performing PSF photometry on the object. In calculating the magnitude of the source in the first, second, and third epochs, we add the template epoch flux to the residual image photometry. The resulting *HST* photometry is given in Table 1.

Figure 5 shows the *HST* photometry along with our *I*- and *z*-band afterglow model (see § 3.2.1) and some early-time data compiled from the GCNs (Ferrero et al. 2004; Hoversten et al. 2004), all corrected for Galactic extinction. By comparing the afterglow

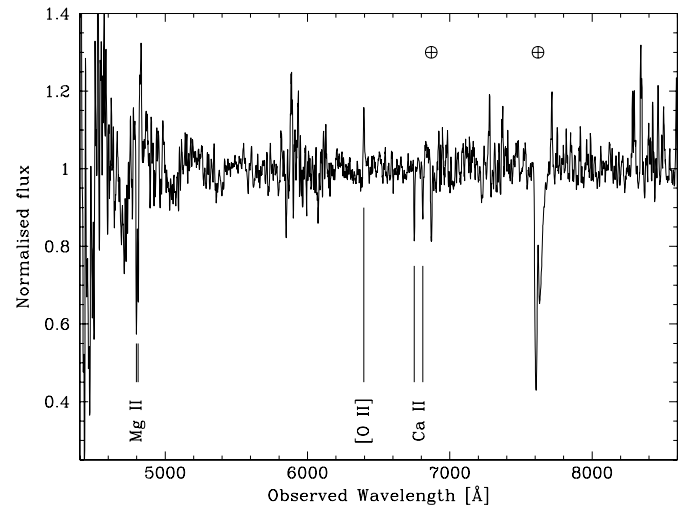


FIG. 3.—Gemini/GMOS spectrum of the optical afterglow for GRB 041006 at $t \approx 0.85$ days. Based on three absorption features and one emission line, we determine the redshift of the host galaxy to be $z = 0.716$, consistent with the earlier report of $z = 0.712$ by Fugazza et al. (2004).

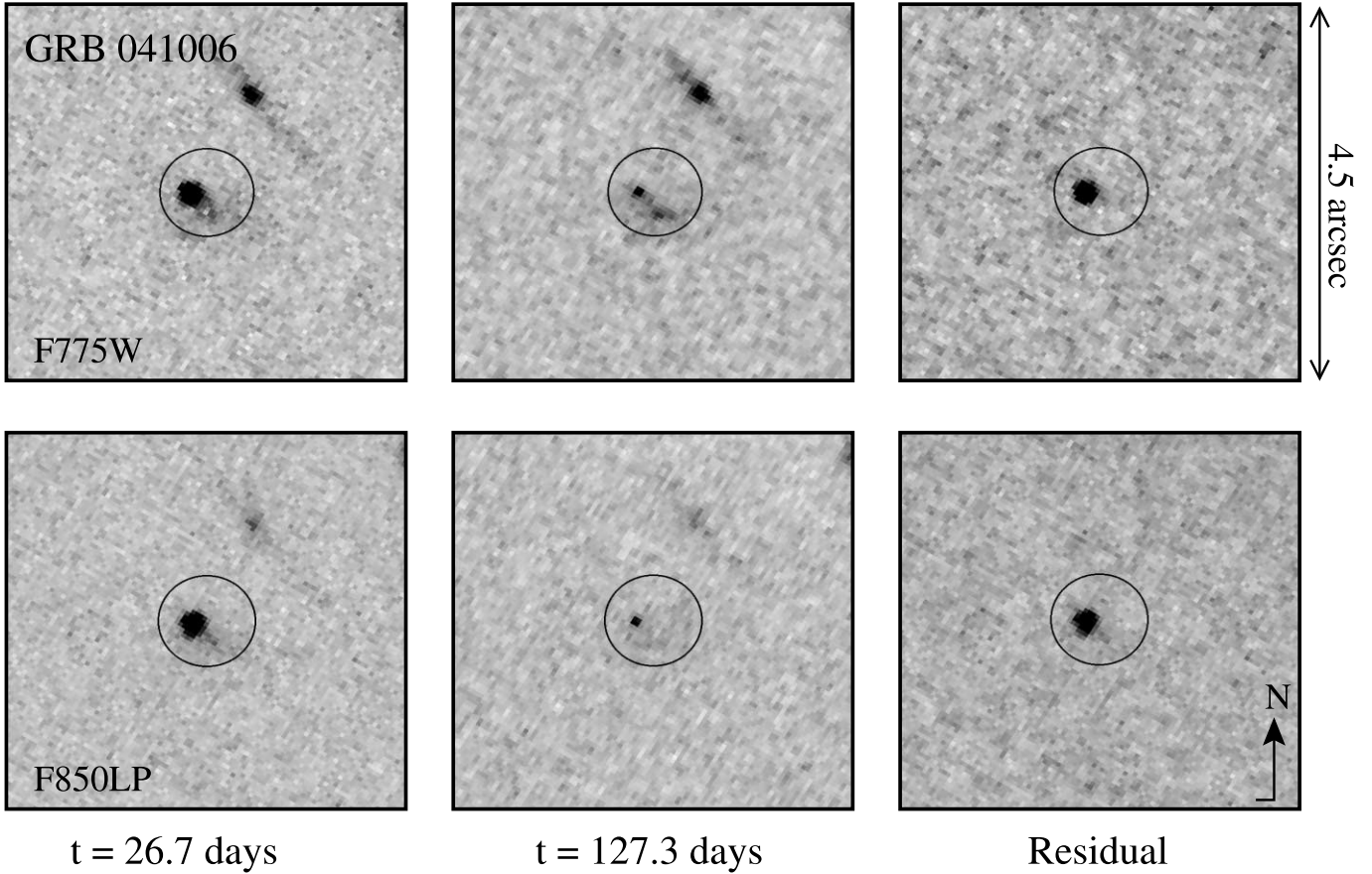


FIG. 4.—Six-panel frame showing *HST* ACS imaging for GRB 041006 at $t \sim 26.7$ days (epoch 1) and $t \sim 127.3$ days (epoch 4) in the F775W and F850LP filters. By subtracting epoch 4 images from those of epoch 1, we produced the residual images shown above. We have applied the same stretch to all frames. As clearly shown in the residual images, a transient source is detected coincident with the $0^{\circ}53$ (2σ) optical afterglow position (circle).

model with the *HST* data, we find evidence for a ~ 2.1 mag rebrightening at $t \sim 27$ days, roughly consistent with the peak time of an SN 1998bw-like SN at $z = 0.71$. We note that this rebrightening was discovered earlier ($t \sim 12$ days) using ground-based facilities and was interpreted as the emerging flux from an associated SN (Bikmaev et al. 2004; Garg et al. 2004; Stanek et al. 2005).

3.2.3. Associated SN

As discussed in § 3.2.1, Stanek et al. (2005) presented an extensive compilation of *R*-band observations that span the epoch of rebrightening. By removing the contribution from the afterglow, they find evidence for an associated SN with a peak magnitude ~ 0.1 mag brighter than SN 1998bw and with a light-curve stretched by a factor of 1.35 in time.

To confirm this result, we compared our redshifted template SN light curves with our late-time *HST* observations and found that an associated SN 1998bw-like SN would be ~ 0.2 mag brighter than the *HST* observation at $t \sim 27$ days, while SN 1994I- and SN 2002ap-like SN light curves are fainter by ~ 1.4 and ~ 2.3 mag, respectively. In an effort to characterize the light curve of the associated SN, we fit the *HST* observations in a manner similar to that done for GRB 040924 (§ 3.1.3). By fitting the *HST* *I*- and *z*-band data simultaneously, we find a best-fit solution ($\chi_r^2 \approx 0.4$) for an SN 1998bw-like SN dimmed by ~ 0.3 mag. We emphasize that this fit does not include any stretching of the light curve. Moreover, we find no improvement in the quality of the fit when template stretching is included. This result is inconsistent with the findings of Stanek et al. (2005). We attribute

this discrepancy to contamination from the host and a nearby galaxy (see Fig. 4), which plagues the Stanek et al. (2005) late-time photometry.

We note that the presence of host galaxy extinction would imply that the associated SN was brighter than our estimates. We use the optical/IR afterglow observations to constrain the host galaxy extinction in a manner similar to that performed for GRB 040924 (§ 3.1.3). However, in this case, the observed spectral index ($\beta_{\text{opt/IR}} \approx -0.5$) is comparable to the theoretical limit and is therefore consistent with negligible host galaxy extinction. We conclude that the SN associated with GRB 041006 was ~ 0.3 mag fainter than SN 1998bw at maximum light and decayed at a comparable rate.

4. DISCUSSION

In the sections above, we showed that GRBs 040924 and 041006 were each associated with a SN similar to SN 1998bw but dimmed by ~ 1.5 and ~ 0.3 mag, respectively. These two events clearly show that there is a significant spread in the luminosity of GRB-associated SNe, suggesting a dispersion in the production of ^{56}Ni . Such a dispersion has already been observed for local SNe Ibc (Richardson et al. 2002).

To better study this dispersion, we compile optical peak magnitudes (rest-frame) and ^{56}Ni mass estimates for GRB/XRF-associated SNe and local SNe Ibc from the literature (Tables 5 and 6). In this compilation we consider all the GRB/XRF-associated SNe with spectroscopic redshifts of $z \lesssim 1$; SN searches at higher redshifts are plagued by UV (rest-frame) line-blanketing. Since spectroscopic confirmation of the SN component is only available

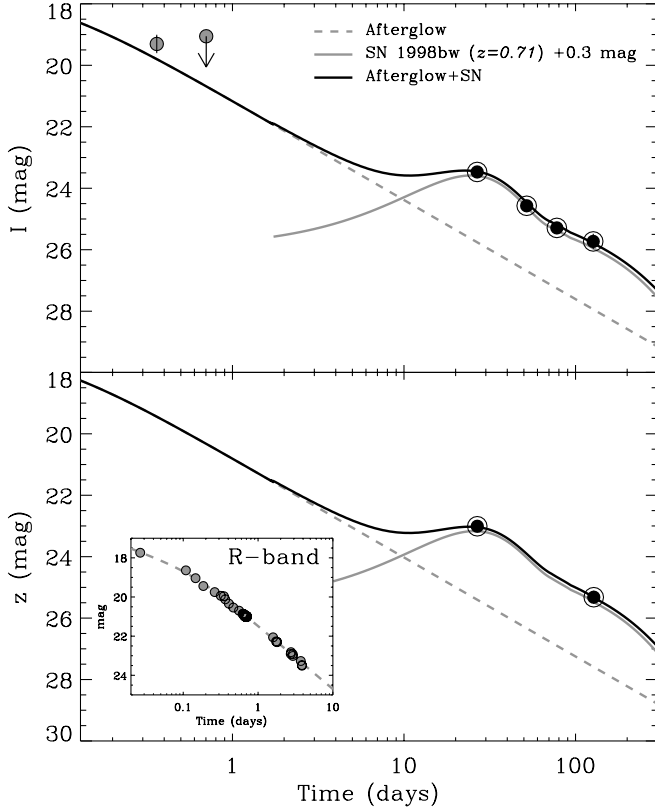


FIG. 5.—Constraints on a SN associated with GRB 041006. Adopting the *R*-band afterglow data reported in Stanek et al. (2005), we reproduce their broken power-law fit (*inset*). Adopting a spectral index of $\beta \approx -0.5$ we then extrapolate the *R*-band afterglow fit to the *I* and *z* bands (gray dashed lines). Extinction-corrected data have been compiled from the GCNs are overplotted (gray circles; Ferrero et al. 2004; Hoversten et al. 2004). We fit the late-time *HST* data (circled dots) by summing the contribution from the afterglow model plus that from a SN. We find a best fit (black solid lines) by including an SN 1998bw-like SN (gray solid lines) redshifted to $z = 0.71$ and dimmed by ~ 0.3 mag.

for the four nearest events in this sample (GRBs 980425, 020903, 031203, and 030329; see Table 5), photometric data is used to constrain the brightness of an associated SN. We note, however, that uncertainty associated with host galaxy extinction and decomposition of the afterglow emission from the SN can impose a nonnegligible uncertainty in the estimated SN peak magnitude. For the local sample, we include only the events with published photometry. The latter may impose a slight bias in favor of brighter and peculiar SNe.¹⁶

In Figure 6 (*top*), we show ^{56}Ni mass estimates and peak optical magnitudes for GRB/XRF-associated SNe and local SNe Ibc. From the figure, it is clear that (1) peak magnitude scales roughly with ^{56}Ni mass, and (2) GRB-associated SNe do not necessarily synthesize more ^{56}Ni than ordinary SNe Ibc.

We next compare their peak optical magnitudes, since the correlation between ^{56}Ni mass and peak optical magnitudes should manifest itself as a similar dispersion. In Figure 6 (*bottom*) we show a histogram of peak optical magnitudes for all GRB/XRF-associated SNe and local SNe Ibc. Examination of the two samples reveals noticeable overlap; while GRB/XRF-associated SNe tend to cluster toward the brighter end of the distribution, some of the faintest SNe Ibc observed are in fact associated with GRBs and XRFs (e.g., GRBs 010921, 040924, and XRF 040701) and the most luminous events are actually drawn from the local sample. Apparently, GRB/XRF-associated SNe are not necessarily over-luminous in comparison with local SNe Ibc. Moreover, by assuming a rough scaling of ^{56}Ni production with peak optical magnitude, this implies a notable overlap between the two samples with respect to their dispersion in synthesized material, consistent with the data shown in the upper panel.

The following question naturally arises: are both GRB/XRF-associated SNe and local SNe Ibc drawn from the same population of events? To address this issue, we performed a Kolmogorov-Smirnov (K-S) test on the two sets of SN peak magnitudes. Our K-S test reveals that the probability the two

¹⁶ Three of the 13 local SNe Ibc included in this compilation were published as “luminous” events. By removing them from the local sample, the probability that both GRB/XRF-associated SNe and local SNe are drawn from the same parent population is reduced to $\sim 50\%$.

TABLE 5
PEAK MAGNITUDES AND ^{56}Ni MASSES FOR GRB- AND XRF-ASSOCIATED SNe

GRB Name	Redshift (z)	$M_{V,\text{peak}}^a$ (mag)	Reference	^{56}Ni Mass (M_\odot)	Reference
GRB 970228.....	0.695	$-18.16^{+0.54}_{-0.52}$	1
GRB 980425.....	0.0085	-19.13 ± 0.05	2	0.6 ± 0.1	3, 4
GRB 980703.....	0.966	$-19.68^{+1.44}_{-0.60}$	1
GRB 990712.....	0.434	$-18.02^{+0.23}_{-0.19}$	1
GRB 991208.....	0.706	$-18.86^{+0.72}_{-0.29}$	1
GRB 000911.....	1.058	$-18.26^{+0.12}_{-0.14}$	1
GRB 010921.....	0.45	< -17.80	5
GRB 011121.....	0.36	$-18.83^{+0.07}_{-0.10}$	1
GRB 020405.....	0.698	$-18.63^{+0.19}_{-0.14}$	1
XRF 020903.....	0.251	-18.53 ± 0.5	6
GRB 021211.....	1.006	$-18.42^{+1.15}_{-0.55}$	1
GRB 030329.....	0.169	-18.83 ± 0.30	7, 8	$0.40^{+0.15}_{-0.10}$	8
GRB 031203.....	0.1055	-19.63 ± 0.15	9
XRF 040701.....	0.2146	< -15.95	6
GRB 040924.....	0.859	-17.63 ± 0.10	10
GRB 041006.....	0.716	-18.83 ± 0.05	10

^a Assuming an SN 1998bw-like light-curve with no additional stretching.

REFERENCES.—(1) Zeh et al. 2004; (2) Galama et al. 1998; (3) Iwamoto et al. 1998; (4) Woosley et al. 1999; (5) Price et al. 2003; (6) Soderberg et al. 2005b; (7) Deng et al. 2005; (8) Lipkin et al. 2004; (9) Malesani et al. 2004; (10) this paper.

TABLE 6
PEAK MAGNITUDES AND ^{56}Ni MASSES FOR NEARBY SNe Ibc

SN Name	$M_{V,\text{peak}}$ (mag)	Reference	^{56}Ni Mass (M_{\odot})	Reference
SN 1983N	-18.89 ± 0.57^a	1	0.25	2
SN 1983V	-18.61 ± 0.41	3
SN 1984L	-18.50 ± 0.10	4	0.20 ± 0.05	5
SN 1987M	-19.40 ± 0.5	6	0.26	7
SN 1990B	-17.91 ± 0.3	8
SN 1991D	-19.6 ± 0.6	9	0.7	9
SN 1992ar	-19.7 ± 0.5	10	$0.5^{+0.25}_{-0.18}$	10
SN 1994I	-17.69 ± 0.58^b	11	0.07 ± 0.035	12
SN 1997ef	-17.1 ± 0.2	13	0.15 ± 0.03	13
SN 1999as	-21.4 ± 0.2	14	4.0 ± 0.5^d	14
SN 1999ex	-17.86 ± 0.26	15	0.16	16
SN 2002ap	-17.4 ± 0.4^c	17	0.07 ± 0.02	18
SN 2003L	-18.18 ± 0.2	19

^a Absolute magnitude brightened by 1.22 mag to be in agreement with the distance assumed by Gaskell et al. (1986).

^b Absolute magnitude dimmed by 0.4 mag to be in agreement with the distance assumed by Iwamoto et al. (1994).

^c Absolute magnitude brightened by 0.2 mag to be in agreement with the distance assumed by Mazzali et al. (2002).

^d Given the similarity of the SN 1999as light-curve to Type II events, it has been suggested that circumstellar interaction contributes to the bright peak luminosity observed for this SN. While there is still no direct indication of such interaction from optical spectra (no narrow emission lines), it is estimated that the explosion must have produced at least $\sim 1 M_{\odot}$ even after correcting for any circumstellar matter interaction (Kasen 2004).

REFERENCES.—(1) Clocchiatti et al. 1996; (2) Gaskell et al. 1986; (3) Clocchiatti et al. 1997; (4) Tsvetkov 1987; (5) Baron et al. 1993; (6) Filippenko et al. 1990; (7) Swartz et al. 1993; (8) Clocchiatti et al. 2001; (9) Benetti et al. 2002; (10) Clocchiatti et al. 2000; (11) Richmond et al. 1996; (12) Iwamoto et al. 1994; (13) Iwamoto et al. 2000; (14) Hatano et al. 2001; (15) Stritzinger et al. 2002; (16) Hamuy et al. 2003; (17) Foley et al. 2003; (18) Mazzali et al. 2002; (19) A. M. Soderberg et al. 2006, in preparation.

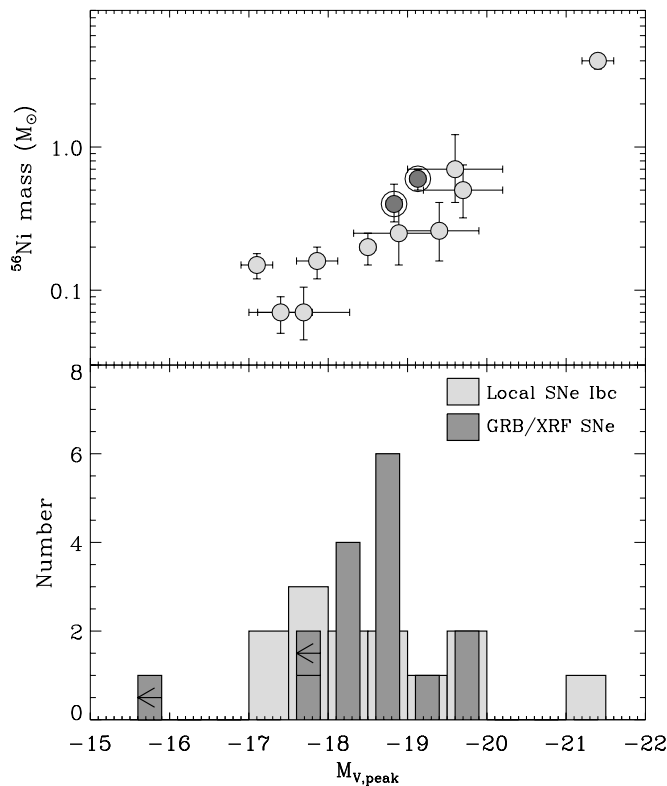


FIG. 6.—*Top*: Rest-frame optical peak magnitudes for GRB-associated SNe (circled dots) and local SNe Ibc (gray circles) have been compiled from the literature (Tables 5 and 6) and are plotted against the mass of ^{56}Ni synthesized in the explosion. For ^{56}Ni estimates without errors, we adopt the fractional uncertainty associated with the peak luminosity. Peak optical magnitudes clearly trace the mass of ^{56}Ni ejected. Apparently, GRB-associated SNe do not necessarily produce more ^{56}Ni than ordinary local SNe Ibc. *Bottom*: Histogram of peak optical magnitudes for GRB/XRF-associated SNe and local SNe Ibc. There is a significant overlap between the two samples. Our K-S test reveals that there is a $\sim 91\%$ probability the two samples are drawn from the same population.

samples have been drawn from the same parent population is $\sim 91\%$. It is therefore conceivable that both SNe Ibc and GRB/XRF-associated SNe belong to the same SN population and thus share a common ^{56}Ni production mechanism.

This result may imply that GRB/XRF-associated SNe and local SNe Ibc share a common progenitor system and/or explosion mechanism. Yet we know from radio observations of local SNe that most Type Ibc SNe lack the engine-driven relativistic ejecta observed in GRBs (Berger et al. 2003; Soderberg et al. 2004, 2005a). This may be accounted for in the spherical+jet paradigm, where the production of ^{56}Ni and relativistic ejecta are independent parameters of the explosion, each of which can be individually tuned. Additional studies of both GRB/XRF-associated SNe and local SNe Ibc will enable us to better map out this two-dimensional parameter space and address in detail the nature of the progenitors and explosion mechanisms.

The authors are grateful for support under the Space Telescope Science Institute grant HST-GO-10135. A. M. S. acknowledges support by the NASA Graduate Student Researchers Program. E. B. is supported by NASA through Hubble Fellowship grant HST-HF-01171.01 awarded by the STScI, which is operated by the Association of Universities for Research in Astronomy, Inc., for NASA, under contract NAS 5-26555. A. G. acknowledges support by NASA through Hubble Fellowship grant HST-HF-01158.01-A awarded by STScI. K. R. is supported by the Gemini Observatory, which provided observations presented in this paper, and which is operated by the Association of Universities for Research in Astronomy, Inc., under a cooperative agreement with the NSF on behalf of the Gemini partnership: the National Science Foundation (United States), the Particle Physics and Astronomy Research Council (United Kingdom), the National Research Council (Canada), CONICYT (Chile), the Australian Research Council (Australia), CNPq (Brazil), and CONICET (Argentina).

REFERENCES

- Alard, C. 2000, *A&AS*, 144, 363
- Baron, E., Young, T. R., & Branch, D. 1993, *ApJ*, 409, 417
- Benetti, S., Branch, D., Turatto, M., Cappellaro, E., Baron, E., Zampieri, L., Della Valle, M., & Pastorello, A. 2002, *MNRAS*, 336, 91
- Berger, E., Kulkarni, S. R., Frail, D. A., & Soderberg, A. M. 2003, *ApJ*, 599, 408
- Beuermann, K., et al. 1999, *A&A*, 352, L26
- Bikmaev, I., et al. 2004, *GCN Circ.* 2826, <http://gc.gsfc.nasa.gov/gcn/gcn3/2826.gcn3>
- Clocchiatti, A., Wheeler, J. C., Benetti, S., & Frueh, M. 1996, *ApJ*, 459, 547
- . 1997, *ApJ*, 483, 675
- Clocchiatti, A., et al. 2000, *ApJ*, 529, 661
- . 2001, *ApJ*, 553, 886
- Covino, S., et al. 2004, *GCN Circ.* 2803, <http://gc.gsfc.nasa.gov/gcn/gcn3/2803.gcn3>
- Da Costa, G., Noel, N., & Price, P. A. 2004, *GCN Circ.* 2765, <http://gc.gsfc.nasa.gov/gcn/gcn3/2765.gcn3>
- Deng, J., Tominaga, N., Mazzali, P. A., Maeda, K., & Nomoto, K. 2005, *ApJ*, 624, 898
- Fenimore, E., et al. 2004, *GCN Circ.* 2735, <http://gc.gsfc.nasa.gov/gcn/gcn3/2735.gcn3>
- Ferrero, P., Bartolini, C., Greco, G., Guarnieri, A., Piccioni, A., Mazzotti Epifani, E., Gualandri, R., & Pizzichini, G. 2004, *GCN Circ.* 2777, <http://gc.gsfc.nasa.gov/gcn/gcn3/2777.gcn3>
- Filippenko, A. V., Porter, A. C., & Sargent, W. L. W. 1990, *AJ*, 100, 1575
- Foley, R. J., et al. 2003, *PASP*, 115, 1220
- Fox, D. 2004, *GCN Circ.* 2741, <http://gc.gsfc.nasa.gov/gcn/gcn3/2741.gcn3>
- Fox, D. W., et al. 2003, *Nature*, 422, 284
- Fruchter, A. S., & Hook, R. N. 2002, *PASP*, 114, 144
- Fugazza, F., et al. 2004, *GCN Circ.* 2782, <http://gc.gsfc.nasa.gov/gcn/gcn3/2782.gcn3>
- Galama, T. J., et al. 1998, *Nature*, 395, 670
- Galassi, M., Ricker, G., Atteia, J.-L., Kawai, N., Lamb, D., & Woosley, S. 2004, *GCN Circ.* 2770, <http://gc.gsfc.nasa.gov/gcn/gcn3/2770.gcn3>
- Garg, A., Stubbs, C., Challis, P., Stanek, K. Z., & Garnavich, P. 2004, *GCN Circ.* 2829, <http://gc.gsfc.nasa.gov/gcn/gcn3/2829.gcn3>
- Gaskell, C. M., Cappellaro, E., Dinerstein, H. L., Garnett, D. R., Harkness, R. P., & Wheeler, J. C. 1986, *ApJ*, 306, L77
- Granot, J., Ramirez-Ruiz, E., & Perna, R. 2005, *ApJ*, 630, 1003
- Hamuy, M., Stritzinger, M., Phillips, M. M., Suntzeff, N. B., Maza, J., & Pinto, P. A. 2003, in *From Twilight to Highlight: The Physics of Supernovae*, ed. W. Hillebrandt & B. Leibundgut (Berlin: Springer), 222
- Hatano, K., Branch, D., Nomoto, K., Deng, J. S., Maeda, K., Nugent, P., & Aldering, G. 2001, *BAAS*, 33, 838
- Heise, J., in 't Zand, J., Kippen, R. M., & Woods, P. M. 2001, in *Gamma-ray Bursts in the Afterglow Era*, ed. E. Costa, F. Frontera, & J. Hjorth (Berlin: Springer), 16
- Henden, A. 2004, *GCN Circ.* 2801, <http://gc.gsfc.nasa.gov/gcn/gcn3/2801.gcn3>
- Hjorth, J., et al. 2003, *Nature*, 423, 847
- Hoversten, E., Chiu, K., Nissen, E., Kelleman, C., & Glazebrook, K. 2004, *GCN Circ.* 2778, <http://gc.gsfc.nasa.gov/gcn/gcn3/2778.gcn3>
- Iwamoto, K., Nomoto, K., Hoflich, P., Yamaoka, H., Kumagai, S., & Shigeyama, T. 1994, *ApJ*, 437, L115
- Iwamoto, K., et al. 1998, *Nature*, 395, 672
- . 2000, *ApJ*, 534, 660
- Kasen, D. 2004, Ph.D. thesis, Univ. California, Berkeley
- Kennicutt, R. C. 1998, *ARA&A*, 36, 189
- Lipkin, Y. M., et al. 2004, *ApJ*, 606, 381
- Li, Z., & Chevalier, R. A. 2003, *ApJ*, 589, L69
- Malesani, D., et al. 2004, *ApJ*, 609, L5
- Matheson, T., et al. 2003, *ApJ*, 599, 394
- Mazzali, P. A., et al. 2002, *ApJ*, 572, L61
- McKenzie, E. H., & Schaefer, B. E. 1999, *PASP*, 111, 964
- Patat, F., et al. 2001, *ApJ*, 555, 900
- Price, P. A., et al. 2003, *ApJ*, 584, 931
- Rhoads, J. E. 1999, *ApJ*, 525, 737
- Richardson, D., Branch, D., Casebeer, D., Millard, J., Thomas, R. C., & Baron, E. 2002, *AJ*, 123, 745
- Richmond, M. W., et al. 1996, *AJ*, 111, 327
- Sari, R., Piran, T., & Halpern, J. P. 1999, *ApJ*, 519, L17
- Sari, R., Piran, T., & Narayan, R. 1998, *ApJ*, 497, L17
- Schlegel, D. J., Finkbeiner, D. P., & Davis, M. 1998, *ApJ*, 500, 525
- Silvey, J., et al. 2004, *GCN Circ.* 2833, <http://gc.gsfc.nasa.gov/gcn/gcn3/2833.gcn3>
- Sirianni, M., et al. 2005, *PASP*, 117, 1049
- Soderberg, A. M., Frail, D. A., & Wieringa, M. H. 2004, *ApJ*, 607, L13
- Soderberg, A. M., Nakar, E., & Kulkarni, S. R. 2005a, preprint (astro-ph/0507147)
- Soderberg, A. M., et al. 2005b, *ApJ*, 627, 877
- Stanek, K. Z., Garnavich, P. M., Nutzman, P. A., Hartman, J. D., & Garg, A. 2005, *ApJ*, 636, L5
- Stritzinger, M. et al. 2002, *AJ*, 124, 2100
- Swartz, D. A., Filippenko, A. V., Nomoto, K., & Wheeler, J. C. 1993, *ApJ*, 411, 313
- Terada, H., & Akiyama, M. 2004, *GCN Circ.* 2742, <http://gc.gsfc.nasa.gov/gcn/gcn3/2742.gcn3>
- Tsvetkov, D. Y. 1987, *Soviet Astron. Lett.*, 13, 376
- Wiersema, K., Starling, R. L. C., Rol, E., Vreeswijk, P., & Wijers, R. A. M. J. 2004, *GCN Circ.* 2800, <http://gc.gsfc.nasa.gov/gcn/gcn3/2800.gcn3>
- Woosley, S. E., Eastman, R. G., & Schmidt, B. P. 1999, *ApJ*, 516, 788
- Yost, S. A., Harrison, F. A., Sari, R., & Frail, D. A. 2003, *ApJ*, 597, 459
- Zeh, A., Klose, S., & Hartmann, D. H. 2004, *ApJ*, 609, 952